Journal of Materials Chemistry B

Dually degradable click hydrogels for controlled degradation and protein release

Journal:	*Journal of Materials Chemistry B*
Manuscript ID:	TB-ART-03-2014-000496.R1
Article Type:	Paper
Date Submitted by the Author:	21-May-2014
Complete List of Authors:	Kharkar, Prathamesh; University of Delaware, Materials Science and Engnieering Kloxin, April; University of Delaware, Chemical & Biomolecular Engineering and Materials Science & Engineering Kiick, Kristi; University of Delaware, Materials Science and Engineering

Dually degradable click hydrogels for controlled degradation and protein release

Prathamesh M. Kharkar,[a] April M. Kloxin,*[ab] and Kristi L. Kiick*[acd]

[a]Department of Materials Science and Engineering, University of Delaware, Newark, DE 19716, USA. E-mail: akloxin@udel.edu; kiick@udel.edu

[b]Department of Chemical and Biomolecular Engineering, University of Delaware, Newark, DE 19716, USA

[c]Biomedical Engineering, University of Delaware, Newark, DE 19716, USA

[d]Delaware Biotechnology Institute, University of Delaware, Newark, DE 19716, USA

1. Introduction

Click reactions have garnered significant interest in the broader areas of materials science and bioconjugation owing to their fast reaction kinetics, high regioselectivity, and efficient reaction yields, all under mild conditions.[1-4] Many click chemistries have been applied to the production of materials, including the traditional azide-alkyne, Diels-Alder, Michael addition, thiol–ene, and oxime reactions.[3, 5] In particular, click reactions that do not require a catalyst or initiator and are free of byproducts, such as the reaction of maleimides and thiols, are useful for biological applications owing to their cytocompatibility in the presence of proteins, cells, or tissues.[6, 7] Utilizing these reactions, injectable hydrogels can be easily created as delivery vehicles for therapeutics, particles, or cells.[8-10] In this application, temporal changes in material properties caused by degradation allow the controlled release of therapeutics, the elaboration of secreted matrix by encapsulated or infiltrating cells, or the spreading, migration, and release of encapsulated cells.[11-13]

Cleavage of the click linkages provides an attractive and relatively cost-effective approach to incorporate degradability without the use of more complex components, such as degradable peptides or proteins. Recent studies have demonstrated the degradability of click crosslinks under mechanical[14, 15] and thermal[16, 17] stresses; however, such reaction conditions can limit the translation of these approaches into clinical applications owing to the limited cytocompatibility of their associated stimuli. Overcoming this limitation, Baldwin

and Kiick have recently introduced thiol-maleimide click reactions in solution and within PEG-heparin hydrogels that are sensitive to reducing microenvironments found *in vivo*.[10, 18] Opportunities to exploit these strategies for controlled delivery of encapsulated cargo molecules, however, have not yet been demonstrated.

Despite recent technological advances, the delivery of therapeutic proteins (e.g., Trastuzumab, Bevacizumab, Rituximab) and small molecule drugs (e.g., Fluorouracil, Paclitaxel) remains a major challenge in the treatment of many diseases, including cancer.[19] In approaches for cancer treatment, delivery to the site of a tumor is critical for therapeutic success and minimization of side effects.[20] Injectable hydrogel-based drug carriers offer advantages for these applications, enabling the efficient encapsulation of cargo molecules while maintaining bioactivity for localized delivery at a preprogrammed rate or responsive manner.[21-24] Depending on the cargo molecule of interest, the rate of release can be controlled by diffusion, degradation, affinity, or a combination of these mechanisms through hydrogel design. Degradation-mediated release is a versatile approach for the temporally controlled delivery of numerous payloads, from hydrophilic proteins to small molecules caged within nanoparticles, without chemical modification of the therapeutic, which can affect drug efficacy and clinical translation.[25-27] Several strategies have been employed to incorporate degradability within the hydrogel by inclusion of labile crosslinks, including esters,[28, 29] photolabile groups,[30-32], and enzyme-sensitive linkers.[25, 33] As will be elaborated below, linkers that are sensitive to reductants are attractive and simple

for controlled release in cancerous tissues, which have elevated levels of sulfur-containing compounds.[34]

Accordingly, reduction-sensitive disulfide linkages have been widely used for intracellular delivery of DNA, siRNA, proteins, and therapeutic drugs.[35-39] These strategies rely on rapid destabilization of the drug carrier due to reduction of disulfide bonds in the presence of glutathione (GSH) tripeptides, one of the major sulfur-containing compounds found at elevated levels within cancerous tissues and cells.[40, 41] Since the intracellular concentration of GSH (ca. 0.5 mM to 10 mM) is 100 to 1000 times higher than the extracellular concentration (ca. 0.001 mM to 0.02 mM), efficient intracellular delivery of cargo molecules has been achieved using disulfide chemistry.[42, 43] However, the rapid rate of degradation of disulfide linkages provides limited control over material degradation and cargo release, and GSH-sensitive linkers that permit controlled extracellular delivery over days to weeks thus have been less explored. In addition, since the concentration of GSH is higher in carcinoma tissues than in healthy tissues due to abnormal proliferative activities of cancer cells,[40, 41, 44] reducing sensitive chemistries incorporated within drug delivery carriers offer great potential for localized cancer treatment. To address this need and opportunity, we present reducing microenvironment-sensitive hydrogels that undergo tunable degradation on the order of days to weeks for controlled protein delivery, demonstrating the broad utility of the click bond cleavage and thiol exchange reaction as a general

strategy not only to control degradation but also to control the release of cargo molecules locally from a bioinert delivery vehicle.

Specifically, we describe the development of multimode, degradable poly(ethylene glycol) (PEG) hydrogels using Michael-type addition and exchange reactions by incorporation of select thioether succinimide crosslinks. These hydrogels are composed of multifunctional PEG crosslinked using thiol-maleimide click chemistry and can undergo degradation by two mechanisms: i) cleavage of click linkages and thiol exchange reactions in the presence of GSH and ii) ester hydrolysis. To achieve this, multiarm PEG macromers were functionalized with different mercaptoacids and reacted with maleimide-functionalized PEG, creating hydrogels that degrade by either hydrolytic *or* hydrolytic and thiol-exchange mechanisms. Hydrogel degradation was monitored in physiologically-relevant GSH microenvironments via oscillatory rheometry and volumetric swelling measurements to assess the degradation kinetics. The ability to incorporate and selectively release a cargo molecule was investigated by monitoring, via fluorescence spectroscopy, the release of bovine serum albumin (BSA) as a model protein. The ability to precisely control hydrogel degradation and thus the release profile of cargo molecules using cleavage of click linkages offers exciting avenues for designing biomaterials for drug delivery and tissue engineering applications.

2. Methods and Materials

2.1 Materials

4-arm hydroxyl-functionalized poly(ethylene glycol) (PEG-4-OH, 10000 g mol^{-1}), 4-arm thiol-functionalized PEG (PEG-4-SH, 10000 g mol^{-1}), and linear maleimide-functionalized PEG (PEG-2-MI, 5000 g mol^{-1}) were purchased from JenKem Technology USA Inc. (Allen, TX). 3-Mercaptopropionic acid (MP), 4-mercaptophenylacetic acid (MPA), p-toluenesulfonic acid monohydrate (PTSA), triethylamine (TEA), dithiothreitol (DTT), and glutathione (GSH) were purchased from Sigma-Aldrich (St. Louis, MO). Trifluoroacetic acid (TFA) and all solvents were obtained from Fisher Scientific (Pittsburgh, PA). Bovine serum albumin labeled with Alexa Fluor 488 (BSA-488) was purchased from Life Technologies (Grand Island, NY). All commercially available reagents were used as received without further purification unless otherwise noted.

2.2 Synthesis of mercaptoacid-based PEG-thiols

PEG was modified with MP or MPA functional groups based on modified versions of previously published protocols.[8, 10] Briefly, PEG-4-OH (0.1 mmol), mercaptoacid (4 mmol), PTSA (0.04 mmol), and toluene (20 mL) were added to an oven-dried round-bottom flask equipped with a reflux condenser. The reaction setup was purged with nitrogen under room temperature. The reaction (**Scheme 1**) was heated to reflux (110 ^{0}C) and stirred for 48 hours, and generated water was collected by using a Dean-Stark trap. Upon completion, the reaction was cooled to room temperature, and the functionalized PEG precipitated three times in ethyl ether. The product was recovered by vacuum filtration and rinsed with 2-propanol

followed by hexane. The dried polymer product (1 equiv) was reduced in toluene using DTT (1 equiv) and TEA (1 equiv) for 5 hours, under inert atmosphere. The finished reaction was acidified with TFA (1.1 equiv), and the polymer was again precipitated in ethyl ether and recovered by filtration. Subsequently, the polymer was dissolved in methanol, and the mixture was filtered through a 0.22 μm filter followed by precipitation in 2-propanol and vacuum filtration. The solid product was rinsed with copious amounts of 2-propanol and hexane. The final dried polymer was obtained by removal of residual solvents under reduced pressure. The degree of thiol functionalization of the polymer was characterized via ^{1}H NMR spectroscopy, using a Bruker AV 400 NMR spectrometer (Bruker Daltonics, Billerica, MA) with $CDCl_3$ as the solvent and TMS as the reference.

PEG-4-MP

The general procedure for synthesis of PEG-thiol was followed using MP as the mercaptoacid to yield PEG-4-MP. The final polymer was obtained as a white solid (0.6 g, 74% yield). The functionality was estimated to be 92% based on integration of the proton neighboring the ester linkage relative to the PEG backbone protons. (**Fig. S1 B**).

^{1}H NMR (400 MHz, $CDCl_3$) δ: 4.28 (8H, t), 3.90-3.35 (900H, bs), 2.82-2.62 (16H, m), 1.68 (4H, t).

PEG-4-MPA

The general procedure for synthesis of PEG-thiol was followed using MPA as the mercaptoacid to yield PEG-4-MPA. The final polymer was obtained as a white solid (0.54 g, 66% yield). The functionality was estimated to be 90% based on integration of the proton neighboring the ester linkage relative to the PEG backbone protons (**Fig. S1 C**).

^{1}H NMR (400 MHz, $CDCl_3$) δ: 7.24-7.08(16H, m), 4.24 (8H, t), 3.90-3.35 (900H, bs), 3.42-3.39 (4H, s).

2.3 Gelation time and rheology characterization

Hydrogel precursor solutions were prepared by dissolution of thiol- and maleimide-functionalized PEG (5% w/w) in citric acid buffer (pH 5) and phosphate-buffered saline (pH 7.4), respectively. Slightly acidic conditions allowed tuning of the gelation time (i.e., increased gelation time) due to the reduced nucleophilicity of thiolate species under acidic conditions;[10, 45] these polymerization conditions previously have been shown to be effective for use in cell/protein studies in vitro.[46] Gelation time was studied qualitatively using the tube inversion method. Briefly, the hydrogel precursor solutions were mixed (100 μL) and immediately pipetted into a glass vial. In five-second intervals, vials were inverted to observe if the solution flowed. The timepoint at which the solution did not flow was recorded as the gelation time.

For rheological studies, the hydrogels were formed directly on the rheometer (AR-G2, TA instruments, USA) by mixing the precursor solutions (1:1

maleimide:thiol molar ratio resulting in 5 % w/w hydrogels), immediately pipetting onto a Peltier plate at 25 ^{0}C, and commencing measurements (120 μm gap). Gelation at room temperature ensured that the gelation time was sufficiently slow to allow good mixing of precursor solutions on the Peltier plate prior to gelation. This also allowed the gels to form homogeneously so that all gels had similar moduli prior to protein release experiments. The gelation time and final shear modulus of the hydrogel were determined using rheometry experiments. Frequency sweeps were performed to determine the linear viscoelastic regime (0.01 to 10 % strain at 6 rad/s). Using a 20-mm diameter parallel plate geometry, time-sweep measurements were obtained within the linear viscoelastic regime (1 % constant strain mode at a frequency of 6 rad/s) at 25 ^{0}C.

2.4 Hydrogel degradation characterization

For hydrogel degradation studies, polymer precursor solutions (5% w/w) were mixed in a 1:1 maleimide:thiol molar ratio and pipetted into a cylindrical mold (diameter = 4.6 mm, thickness = 1.8 mm). The solutions were allowed to gel for two hours at room temperature to ensure maximum possible crosslink density was achieved for all samples. The rheological data showed that once the gels have been formed (i.e., stable storage moduli is achieved at 30 min), the moduli remain consistent through 2 hours. The resulting hydrogels were washed with PBS and incubated, at room temperature, in 5 mL of PBS buffer (pH 7.4) containing GSH (0 mM, 0.01 mM or 10 mM) over the experimental time period. The pH of the buffer after GSH addition was adjusted to a pH of 7 by addition of 0.1 M sodium

hydroxide. Degradation was monitored by measuring volumetric swelling and shear modulus. For the shear modulus measurements, time sweeps were performed within the linear viscoelastic regime for each sample (2 rad/s, 2% strain, and 0.25 N normal force in order to prevent hydrogel slip).

2.5 Volumetric swelling and mesh size calculations

Hydrogel discs (diameter = 4.6 mm, thickness = 1.8 mm) were placed in PBS buffer with 0 mM, 0.01 mM, or 10 mM GSH at room temperature and gently rocked. Samples were removed at respective time points, and the diameters of hydrogels were measured using a Vernier caliper, whereas the height was determined using the rheometer gap values. Volume of the hydrogel at each time points was determined based on measured diameter and height and assuming cylindrical geometry. The % volumetric swelling at each time point was calculated by normalizing to the volume of the gel immediately after formation (day 0 before equilibrating with PBS).

2.6 Protein release

For protein release experiments, polymer precursor solutions (5% w/w) were mixed in a 1:1 maleimide:thiol molar ratio along with BSA-488 (loading concentration 1.2 mg/ml) and added to a cylindrical mold (diameter = 4.6 mm, thickness = 1.8mm). The solutions were allowed to gel for two hours at room temperature. Hydrogel discs were immediately washed with PBS thrice to remove any non-encapsulated BSA-488 and then gently rocked at room temperature in 5

mL of PBS buffer with GSH (10 mM). The amount of BSA-488 present in the hydrogel was calculated by subtracting the amount of BSA-488 released during wash steps from the amount of BSA-488 that was initially loaded into the gel. At each time point, a 100-μL aliquot of the sink solution was removed for protein release measurements and replaced by 100 μL of fresh GSH in PBS. The released BSA-488 was quantified by fluorescence measurements using a microplate reader (Synergy H4, BioTek Inc., Winooski, VT) taking into account the cumulative sample dilution due to removal and addition of fresh GSH in PBS at each time point measurement (see Supporting Information). To estimate the concentration of released BSA-488, a calibration curve for the fluorescence of BSA-488 as a function of its concentration was acquired. The release of the BSA was monitored via SDS-PAGE analysis of the solutions removed at each timepoint; 7 μL of sink solution containing released protein was loaded onto a standard sodium dodecyl sulfate-polyacrylamide gel electrophoresis (SDS-PAGE) for analysis. The concentration of protein in each band was quantified with densitometry analysis using the gel analysis function in ImageJ (version 1.46).

2.7 Statistical analysis

Results are expressed as mean ± standard error of mean (SEM) unless otherwise specified. Monomer synthesis reactions were performed in duplicate. Hydrogel formation experiments were performed in triplicate. Degradation and protein release studies were performed in duplicate with 3 hydrogels per condition at each

experimental time point. Statistical comparisons were based on analysis of variance (ANOVA) and $p < 0.05$ was considered statistically significant.

3. Results and Discussion

3.1 Hydrogel compositions for control of degradation

Many natural and synthetic polymers have been used for hydrogel formation, with polymer selection partly dictated by the application of interest.[5] PEG-based hydrogels are well suited for drug delivery applications owing to their biocompatibility, lack of protein binding sites, and the ease of engineering their properties.[47] The facile functionalization of the hydroxyl end groups of PEG allows the incorporation of different chemical functionalities for hydrogel formation in the presence of proteins and cells *and* for controlled degradation. Exploiting these advantages, PEG-OH was functionalized with alkyl (MP) and aryl (MPA) based mercaptoacids utilizing established protocols.[8, 10] These thiol end groups act as nucleophiles and react rapidly with maleimide functional groups to form crosslinks by a Michael-type addition reaction. Michael-type addition reactions are highly efficient and versatile reactions that occur under physiological conditions without byproducts and have been used to crosslink cytocompatible hydrogels.[48-50] Here, the composition of the hydrogel was varied to enable microenvironment-controlled degradation and protein release (**Fig. 1**). PEG-4SH-based hydrogels (**Control**), which contain water stable ether bonds, served as a non-degradable control owing to lack of any degradable functional groups. Owing to the presence of ester linkages, MP-based hydrogels (one

degradable group, **D1E**) undergo ester hydrolysis, whereas the MPA-based hydrogels (two degradable groups, **D2ER**) undergo ester hydrolysis and click bond cleavage and thiol exchange reactions.

3.2 Consistent hydrogel formation

Dynamic time sweep experiments were conducted to study hydrogel gelation kinetics and final hydrogel moduli. Data were acquired within the linear viscoelastic regime. After vortexing the precursor solutions, the storage and loss moduli were recorded as a function of time. Representative results for the **D2ER** hydrogel formation are shown in **Fig. 2A**. The crossover point (i.e., G'=G"), which is an indirect measurement of the gel point, was not observed due to the rapid onset of gelation before the first data point was acquired; the gelation time thus was semi-qualitatively determined by the tube inversion method.[51] Faster gelation was observed for **D2ER** (~20 sec) compared to **D1E** (~35 sec) and **Control** (~40 sec) hydrogels; this rapid gelation is consistent with the reported kinetics of thiol-maleimide reactions.[52] The time difference for gelation between **D2ER**, **D1E**, and **Control** can be attributed to the thiol reactivity (**D1E** and **Control**, alkylthiols pK_a = 10.2; **D2ER**, arylthiols pK_a = 6.6).[53, 54] The difference in thiol reactivity of **Control**, **D1,** and **D2ER** essentially arises from the mesomeric effect provided by the aromatic ring in the case of **D2ER,** making it more nucleophilic than **Control** and **D1E**.

Presence of aromatic ring in **D2ER** results in higher nucleophilicity due to mesomeric effect, which dictates the thiol reactivity. With increasing time, the storage modulus (G') increases rapidly without a significant increase in loss modulus (G"). These data highlight the elastic nature of the network. Time to achieve final storage moduli varied depending upon the identity of thiol groups, which again can be attributed to the thiol reactivity (**D2ER**: ~15 minutes; **D1E**: ~30 min; and **Control**: ~34 min). Although the experiments were performed at the room temperature (25 ^{0}C), the gelation time and time to achieve the final storage moduli can be further decreased by forming hydrogels at elevated temperatures.

Material modulus is directly correlated with the crosslink density as per the theory of rubber elasticity.[55] The final storage moduli, which is defined as the value of G' after reaching plateau, for **Control**, **D1E**, and **D2ER** hydrogels were examined to compare the consistency in crosslink density between the different compositions (**Fig. 2B**). The final post-gelation, equilibrium-swollen G' were recorded after complete gelation for **Control**, **D1E**, and **D2ER**. As indicated in the figure, the post gelation equilibrium G' was ~2.3 kPa for all three compositions. There were no statistically significant differences between the final plateau moduli of the various gels (one-way ANOVA, $p = 0.88$), indicating that the use of different thiols did not affect the final crosslink density substantially. Side reactions such as disulfide formation and maleimide ring hydrolysis alter the reactivity of the thiol and maleimide groups and thus could affect the number of functional groups

available for hydrogel formation (**Scheme S1**), potentially decreasing the final moduli for a particular composition. The lack of a statistically significant difference between the final equilibrium G' values thus also suggests that there were no significant differences in the extent of these side reactions for the various hydrogel compositions. These results suggest that differences in gelation for **Control**, **D1E**, and **D2ER** did not significantly contribute to network defects due to strict 1:1 stoichiometry and relative rate of Michael-type addition as compared to other defect forming side reactions. Further, the molecular weight of the PEG chains for the gel compositions investigated here was selected to minimize any looping, unreacted functionalities, and other related network defects based on studies of related PEG hydrogels in the literature.[45] The similarity of the initial crosslink densities between the **Control**, **D1E**, and **D2ER** hydrogels allow the study of the degradation kinetics by direct monitoring of changes in G' as a function of time.

3.3. Degradation in a reducing microenvironment

In order to evaluate the most rapid hydrogel degradation that might be observed in physiologically relevant reducing microenvironments, as well as to evaluate the associated degradation mechanism, the higher GSH of 10 mM first was examined. Potential degradation mechanisms for each hydrogel composition are described in **Fig. 3**. Thioether succinimide linkages formed using arylthiols (**D2ER** hydrogels) can undergo thiol exchange in the presence of exogenous thiols (a GSH-rich microenvironment) in contrast to alkylthiols (**Control** and **D1E**), which are stable

within the experimental time frame (stable at t < 6 days).[18] The presence of ester linkages in the **D1E** and **D2ER** hydrogels allows degradation by ester hydrolysis over longer time scales (stable at t > 1 month to 2 years depending upon neighboring groups).[56] A potential hindrance to degradation by the thiol exchange mechanism is possible hydrolysis of the maleimide ring, which leads to ring opening and the formation of an irreversible crosslink. However, the rate of maleimide ring hydrolysis is significantly slower (by one order of magnitude) than the competing click cleavage and thiol exchange reaction ($k = 3.7 \times 10^{-2}\ h^{-1}$ for click cleavage and thiol exchange, $k = 3.3 \times 10^{-3}\ h^{-1}$ for maleimide ring hydrolysis).[18] Consequently, we assume that changes in G' for **D2ER** hydrogels are dominated by mainly thiol-exchange reactions in reducing microenvironments and by ester hydrolysis in non-reducing microenvironments.

Oscillatory rheometry and volumetric swelling measurements were used to study the degradation of the hydrogels (defined here as the scission of network crosslinks) under thiol-rich reducing conditions. Degradation kinetics were assessed by measuring the storage moduli of hydrogel discs that were suspended in solutions containing 10 mM GSH (**Fig. 4A**). The storage moduli at each time point were normalized to the initial modulus for that gel composition directly after formation (day 0 before equilibrating with PBS), where the initial gel has a normalized modulus of 100%. As illustrated in the figure, the **Control** and **D1E** samples exhibited an initial decrease in G' to approximately 80% of the normalized value within 24 hours, but did not exhibit any further rapid decrease in

moduli after this point. The initial decrease can be attributed to the equilibrium swelling that occurs after hydrogel formation. No significant change was observed in G' post-equilibrium swelling for **Control** hydrogels, which was expected since no degradable functional groups are present within these hydrogels. A slight decrease in modulus over time was observed for **D1E** hydrogels, which can be attributed to ester hydrolysis (calculated first-order rate constant, $k = 3.33 \times 10^{-5}\ min^{-1}$). This rate constant compares well with the typical ester linkage hydrolysis rate constant in hydrophilic polymer networks (1.33×10^{-5} to $7.33 \times 10^{-6}\ min^{-1}$) corresponding to half lives of 6 to 32 days.[57] The degradation rate constant for **D1E** was found to be statistically different from the **Control** (two-tailed P value = 0.005), highlighting the role of ester linkages in the degradation of **D1E (Fig. S3 and S4).** In contrast, a rapid decrease in G' was observed for **D2ER** hydrogels, and the reverse gel point, defined as complete hydrogel dissolution, was observed after approximately 4 days (at 5700 minutes). The rapid decrease in G' indicates a substantial decrease in crosslink density and can be attributed to the reversibility of the thiol-maleimide reaction and the consequent thiol exchange reactions that occur in the presence of GSH. As the rates of ester hydrolysis and maleimide ring hydrolysis are slow, the rapid rate of degradation of **D2ER** highlights the role of click bond cleavage and thiol exchange reaction as leading cause of hydrogel degradation.

Temporal changes in the volumetric swelling also were examined for the **Control**, **D1E**, and **D2ER** hydrogels that were suspended in 10 mM GSH (**Fig. 4B**). All

three hydrogel compositions showed an initial increase in the swelling as the hydrogels achieved equilibrium swelling. The **Control** and **D1E** hydrogels remained stable after this initial swelling event (t > ~24 hours), whereas the volumetric swelling for **D2ER** hydrogels continued increasing until complete degradation (gel dissolution) occurred at 5700 minutes. The continuous increase in the swelling before complete degradation for **D2ER** is consistent with a bulk degradation mechanism, as well as with the rheometric measurements where the increases in swelling are commensurate with observed decreases in modulus. Overall, these results indicate that well-defined hydrogels can be designed to degrade in a reducing microenvironment with selection of arylthiol-based thioether succinimide linkages. Such a system could prove useful in the design of hydrogels for controlled and local delivery of anti-cancer drugs.

3.4 Influence of GSH concentration on hydrogel degradation

To reject the possibility that the degradation of **D2ER** hydrogels under high [GSH] conditions was substantially affected by ester hydrolysis, the mechanical properties of **D2ER** hydrogels were monitored in solutions lacking GSH (0 mM GSH). In addition, since thiol exchange reactions are dependent on GSH concentration, we investigated an additional condition (0.01 mM GSH, **D2ER** hydrogel), which mimics the extracellular GSH concentration. The storage moduli (G') of hydrogels were measured at predetermined time points. The **Control** hydrogel exhibited an initial decrease in G' over the first 24 hours, after which G' did not change, irrespective of GSH concentration (0 and 10 mM, **Fig. S3**). As

discussed in Section 3.3, the initial changes in G' can be attributed to equilibrium swelling. The constant moduli observed for timepoints after 24 hours indicate that the polymeric crosslinks are stable within the experimental timeframe and do not undergo any significant degradation. For **D1E** hydrogels, the storage moduli initially decreased, which again can be attributed to equilibrium swelling (**Fig. S4**). However, for the **D1E** hydrogel, the decrease in storage moduli continued past 24 hours, which would be consistent with degradation via ester hydrolysis as discussed above.

As shown in **Fig. 5**, the storage moduli varied as a function of GSH concentration for **D2ER** hydrogels. For the 0 mM GSH condition, G' initially decreased during the first 24 hours, owing to equilibrium swelling, followed by a slow decrease in G' to 81% of its initial normalized value. The decrease after 24 h can be attributed to ester hydrolysis ($k = 1.35 \times 10^{-5}$ min^{-1}, $t_{1/2} = 35$ days). For 0.01 mM GSH, G' decreases rapidly and complete gel degradation was observed at approximately 8 days (t ~200 h), indicating that the degradation mechanism in the presence of glutathione is dominated by the reversibility of the thiol-maleimide reaction and the resulting thiol exchange that is possible in the presence of GSH. Further, in comparison with solutions containing 10 mM GSH, these data highlight the dependence of the rate of **D2ER** hydrogel degradation on GSH concentration. At lower GSH concentration, the free thiol groups (~14 μM) generated due to the click bond cleavage compete with the free GSH thiols (~10 μM), since the concentration is comparable. In this case, the GSH concentration is a limiting

factor, and the rate of degradation is significantly slower for 0.01 mM compared to the 10 mM GSH condition, in which GSH is present in a large excess. Overall, these results indicate that the **D2ER** hydrogels can undergo ester hydrolysis, but the rate of ester hydrolysis is very slow (under 0 mM GSH k ~ 10^{-5} min^{-1}). As rapid degradation of D2ER hydrogels is observed under reducing conditions (10 mM GSH k ~ 10^{-3} min^{-1}), the data clearly indicate that the click bond cleavage and thiol exchange reaction is the primary mechanism for gel degradation. Further, to verify that **D2ER** hydrogels can undergo complete degradation via ester hydrolysis, **D2ER** hydrogels were subjected to basic conditions to accelerate ester bond hydrolysis (0.1 M sodium carbonate buffer, pH 11.5) and exhibited complete degradation within 24 hours in the absence of a reducing microenvironment, confirming the dual degradability of the hydrogels.

To further investigate the mode of degradation, temporal changes in the volumetric swelling were monitored for **D2ER** hydrogels suspended in various reducing microenvironments (**Fig. 5B**). During the first 24 hours, the volumetric swelling increases for all three conditions, which can be attributed to initial hydrogel equilibrium swelling. After 24 hours, the volumetric swelling continuously increases for the 0.01 mM and 10 mM condition over the course of degradation, which is consistent with rheometric measurements. A bulk degradation mechanism is indicated by this continuous increase in the swelling as a function of time.[25, 58]

3.5 Degradation Kinetics

Regression analysis was conducted to obtain further insight into the degradation mechanism of **D2ER** hydrogels and the kinetics of associated degradation reactions (**Fig. 6**). When exposed to 0 mM GSH, the decrease in storage moduli can be attributed to ester hydrolysis. Owing to the highly swollen nature of the hydrogels, and since the buffer is present in large excess, the water concentration during the degradation time period can be assumed to be relatively constant. Hence, the reaction kinetics was observed to be pseudo-first order with a rate constant $1.87 \times 10^{-5} \pm 5.83 \times 10^{-6}$ min^{-1}. The differences in the rate of ester hydrolysis calculated for the **D2ER** (here) and **D1E** hydrogels (above) can be attributed to local hydrophobic domains associated with aryl thiols in the **D2ER** gels, consistent with a previously reported study by Schoenmakers *et al.* in which the rate of ester hydrolysis varied with local hydrophobicity.[59] When **D2ER** gels were exposed to 0.01 mM GSH, a rapid decrease in G' was observed, consistent with the occurrence of both thiol exchange reactions and ester hydrolysis. Because the theoretical concentration of thiol groups from PEG is comparable to that of the thiol groups from GSH (see above), the rate of hydrogel degradation is dependent both on the concentration of degradable functional groups (which correlate with the crosslink density with 2 degradable groups per crosslink) and the concentration of GSH. Consistent with this, the hydrogel degradation kinetics were observed to be second order, with a rate constant $5.03 \times 10^{-6} \pm 0.16 \times 10^{-6}$ mM^{-1} min^{-1}. With a higher concentration of GSH, the **D2ER** hydrogel rapidly degrades. At 10 mM GSH, the GSH is present in large excess (~3 orders of

magnitude as compared to thiols present in the hydrogel), and thus the concentration of GSH can be assumed to be constant during the experimental time frame. Thus, the rate of degradation is dependent on only the crosslink density, and first order degradation kinetics regression analysis yields a rate constant of $1.75 \times 10^{-3} \pm 0.26 \times 10^{-3}$ min^{-1}. The degradation rate constants for the **Control**, **D1E**, and **D2ER** hydrogels are been summarized in **Table S1**.

3.6 Controlled release of a model protein

The ability to tune the rate of degradation by varying crosslink chemistry offers opportunities to utilize these hydrogels for the controlled release of therapeutics in response to the reducing microenvironment or at a preprogrammed rate by ester hydrolysis. To study the applicability of these hydrogels for controlled release applications, a fluorescently-tagged model protein, bovine serum albumin (BSA-488), was encapsulated during hydrogel formation. BSA-488 was chosen as a model protein for release studies since the hydrodynamic diameter (~ 7.2 nm)[60] is comparable to the estimated hydrogel mesh size (~ 9 nm). The size of the BSA and mesh size calculated for the hydrogels suggest that these materials would be useful for tailored release by hydrogel degradation, upon which the mesh size becomes large enough to facilitate protein release. Similarly, bioactive proteins (e.g., growth factors), therapeutic-laden nanoparticles, or even cells could be released by this mechanism.

The release of BSA-488 was monitored by measuring fluorescence as a function of time. The percent cumulative release was plotted as a function of time for all three compositions (**Fig. 7A**). Approximately 40 % of BSA-488 was initially released from all hydrogel compositions (**Control**, **D1E**, and **D2ER** hydrogels). This release may be attributed to the increase in mesh size associated with initial equilibrium swelling. The effective diffusion coefficient (D_e) was calculated using a modified form of Fick's law[61, 62] and the value was found to be ~ 1.56 x 10^{-8} cm^2 sec^{-1} (see Supporting Information). This value of D_e is in agreement with previously reported D_e values for BSA release from PEG hydrogels.[63] **D2ER** hydrogels, which undergo rapid degradation in reducing microenvironments owing to thiol exchange reactions, exhibited degradation-dependent release, with ~95 % of the cargo released after approximately 4 days, commensurate with when complete hydrogel degradation was observed. This result suggests that the degradation reaction broadly modulates the release of the cargo molecule. Here, the D_e was found to be 5.70 x 10^{-8} cm^2 sec^{-1}. The difference between the effective diffusion coefficients for the hydrogel compositions correlates with the degradation profile of these hydrogels.

SDS PAGE was employed to assess the molecular mass of the released BSA as an indirect measure of its stability during encapsulation and release from the various hydrogel compositions (**Fig. 7B**). Lanes 2 and 3 in the figure, which served as controls, were loaded with BSA-488 in PBS buffer containing 10 mM GSH prepared at two different time points (i.e., just before electrophoresis and before

starting the release experiment for BSA-488, respectively). Lane 4, 5, and 6 were loaded with sink solution containing released BSA-488 from the **Control**, **D1E**, and **D2ER** hydrogels, respectively. No major differences were observed between the band locations. These results suggest that there were no substantial changes in the overall hydrodynamic volume or molecular weight of the protein during encapsulation and release. Densitometry analysis was carried out using NIH Image J software. The band intensity from lane 3 was normalized to 100%, and compared with the band intensity of released BSA from the **Control** (~33%), **D1E** (~36%), and **D2ER** (~90%) hydrogels. The results correlated well with the protein release data obtained using fluorescence measurements. Taken together, these results suggest the utility of GSH-responsive hydrogels as a drug carrier for controlled cargo release applications. However, for applications where rapid release (~1 to 3 hours) of cargo is desired in response to reducing microenvironment, disulfide linkages still may be more appropriate.

Few studies have reported the use of dually degradable hydrogels for tissue engineering and cell encapsulation applications,[28, 64] and the use of dually degradable hydrogels for controlled release applications has been limited. Recently, Wang and co-workers investigated use of dually degradable hydrogels for protein release studies by incorporating an enzymatically degradable hyaluronic acid based backbone and chemically cleavable disulfide linkages.[65] Depending on concentration of hyaluronidase and GSH, the hydrogel exhibited significant degradation within the first ~1.5 to 5 hours, and complete release of a

cargo molecule (stromal cell-derived factor 1α, 100 ng) was achieved within approximately 8 hours. The click cleavage and subsequent thiol exchange system presented here undergoes degradation on a significantly longer timescale (~ 4 days) offering advantages for controlled drug delivery, where wider control over degradation can help transition to clinical applications. In addition, incorporation of ester linkages affords long term clearance of these hydrogels from *in vivo* microenvironments due to ester hydrolysis and subsequent degradation.

4. Conclusions

In this work, we report dually degradable PEG hydrogels in which degradation can be tailored, without affecting hydrogel formation, by the Michael-type addition of select functional groups that yield crosslinks with tunable, and previously unexplored, degradation mechanisms. This facile approach enables hydrogel formation by broadly useful thiol-maleimide click chemistry employing arylthiols, while eliminating the need for the additional incorporation of more complex and potentially costly labile chemistries within the crosslinker to facilitate degradation, such as enzyme-labile peptides. The rate of hydrogel degradation was found to be dependent upon the chemistry of linker, the number of degradable crosslinks, and the concentration of the reducing microenvironment. The release of a model protein from these hydrogels demonstrates the potential of these matrices and approaches for controlled release applications in thiol-rich reducing microenvironments. Control of degradation rates permitted a 2.5-fold difference in protein release for the dually degradable

(**D2ER**) as compared to the non-degradable (**Control**) or single-mode degradable (**D1E**) hydrogels. In principle, this strategy could easily be employed for controlled release over different time frames using combinations of these thiol functional groups within a single hydrogel or utilized in conjunction with more elaborate degradable chemistries when desired for more complex degradation and release profiles. The degradation of hydrogels by cleavage of click linkages presents considerable opportunities in the design of materials for controlled drug delivery and soft tissue engineering applications.

5. Acknowledgements

Research reported in this publication was supported by Institutional Development Award (IDeA) from the National Institute of General Medical Sciences of the National Institutes of Health under grant number P20GM103541 and the University of Delaware Research Foundation. The authors thank Dr. Wilfred Chen for use of the plate reader. The authors thank Rachel Kennel for technical help with precursor solution and hydrogel preparation. Additionally, the authors would like to thank Matthew Rehmann, Megan Smithmyer, Lisa Sawicki, and Kelsi Skeens for feedback on earlier versions of this manuscript.

6. References

1. J. E. Moses and A. D. Moorhouse, *Chem Soc Rev*, 2007, 36, 1249-1262.
2. R. Manetsch, A. Krasinski, Z. Radic, J. Raushel, P. Taylor, K. B. Sharpless and H. C. Kolb, *J Am Chem Soc*, 2004, 126, 12809-12818.
3. C. M. Nimmo and M. S. Shoichet, *Bioconjug Chem*, 2011, 22, 2199-2209.
4. H. C. Kolb, M. G. Finn and K. B. Sharpless, *Angew Chem Int Ed Engl*, 2001, 40, 2004-2021.
5. P. M. Kharkar, K. L. Kiick and A. M. Kloxin, *Chem Soc Rev*, 2013, 42, 7335-7372.
6. R. J. Pounder, M. J. Stanford, P. Brooks, S. P. Richards and A. P. Dove, *Chem Commun*, 2008, 5158-5160.
7. M. A. Azagarsamy and K. S. Anseth, *ACS Macro Lett*, 2013, 2, 5-9.
8. T. Nie, A. Baldwin, N. Yamaguchi and K. L. Kiick, *J Control Release*, 2007, 122, 287-296.
9. H. Wang, A. Han, Y. Cai, Y. Xie, H. Zhou, J. Long and Z. Yang, *Chem Commun*, 2013, 49, 7448-7450.
10. A. D. Baldwin and K. L. Kiick, *Polym Chem*, 2013, 4, 133-143.
11. M. W. Tibbitt, B. W. Han, A. M. Kloxin and K. S. Anseth, *J Biomed Mater Res A*, 2012, 100, 1647-1654.
12. C. Adelow, T. Segura, J. A. Hubbell and P. Frey, *Biomaterials*, 2008, 29, 314-326.
13. F. P. Brandl, A. K. Seitz, J. K. Tessmar, T. Blunk and A. M. Gopferich, *Biomaterials*, 2010, 31, 3957-3966.
14. J. N. Brantley, K. M. Wiggins and C. W. Bielawski, *Science*, 2011, 333, 1606-1609.
15. K. M. Wiggins, J. N. Brantley and C. W. Bielawski, *Acs Macro Letters*, 2012, 1, 623-626.
16. T. Dispinar, R. Sanyal and A. Sanyal, *J Polym Sci A Polym Chem*, 2007, 45, 4545-4551.

17. K. C. Koehler, K. S. Anseth and C. N. Bowman, *Biomacromolecules*, 2013, 14, 538-547.
18. A. D. Baldwin and K. L. Kiick, *Bioconjug Chem*, 2011, 22, 1946-1953.
19. D. S. Dimitrov, *Methods Mol Biol*, 2012, 899, 1-26.
20. K. K. Jain, in *Applications of Biotechnology in Oncology*, Springer, 2014, pp. 617-669.
21. B. V. Slaughter, S. S. Khurshid, O. Z. Fisher, A. Khademhosseini and N. A. Peppas, *Adv Mater*, 2009, 21, 3307-3329.
22. T. R. Hoare and D. S. Kohane, *Polymer*, 2008, 49, 1993-2007.
23. Y. Li, J. Rodrigues and H. Tomas, *Chem Soc Rev*, 2012, 41, 2193-2221.
24. T. Vermonden, R. Censi and W. E. Hennink, *Chem Rev*, 2012, 112, 2853-2888.
25. A. A. Aimetti, A. J. Machen and K. S. Anseth, *Biomaterials*, 2009, 30, 6048-6054.
26. Y. Fu and W. J. Kao, *Expert Opin Drug Deliv*, 2010, 7, 429-444.
27. T. Diab, E. M. Pritchard, B. A. Uhrig, J. D. Boerckel, D. L. Kaplan and R. E. Guldberg, *J Mech Behav Biomed Mater*, 2012, 11, 123-131.
28. S. Sahoo, C. Chung, S. Khetan and J. A. Burdick, *Biomacromolecules*, 2008, 9, 1088-1092.
29. M. S. Rehmann, A. C. Garibian and A. M. Kloxin, *Macromol Symp*, 2013, 329, 58-65.
30. A. M. Kloxin, A. M. Kasko, C. N. Salinas and K. S. Anseth, *Science*, 2009, 324, 59-63.
31. A. M. Kloxin, M. W. Tibbitt, A. M. Kasko, J. A. Fairbairn and K. S. Anseth, *Adv Mater*, 2010, 22, 61-+.
32. D. R. Griffin, J. L. Schlosser, S. F. Lam, T. H. Nguyen, H. D. Maynard and A. M. Kasko, *Biomacromolecules*, 2013, 14, 1199-1207.
33. J. Patterson and J. A. Hubbell, *Biomaterials*, 2010, 31, 7836-7845.
34. G. K. Balendiran, R. Dabur and D. Fraser, *Cell Biochem Funct*, 2004, 22, 343-352.

35. F. Meng, W. E. Hennink and Z. Zhong, *Biomaterials*, 2009, 30, 2180-2198.
36. R. Cheng, F. Feng, F. Meng, C. Deng, J. Feijen and Z. Zhong, *J Control Release*, 2011, 152, 2-12.
37. X. J. Cai, H. Q. Dong, W. J. Xia, H. Y. Wen, X. Q. Li, J. H. Yu, Y. Y. Li and D. L. Shi, *J Mater Chem*, 2011, 21, 14639-14645.
38. J. Liu, Y. Pang, W. Huang, X. Huang, L. Meng, X. Zhu, Y. Zhou and D. Yan, *Biomacromolecules*, 2011, 12, 1567-1577.
39. H. Y. Wen, H. Q. Dong, W. J. Xie, Y. Y. Li, K. Wang, G. M. Pauletti and D. L. Shi, *Chem Commun*, 2011, 47, 3550-3552.
40. E. Ferruzzi, R. Franceschini, G. Cazzolato, C. Geroni, C. Fowst, U. Pastorino, N. Tradati, J. Tursi, R. Dittadi and M. Gion, *Eur J Cancer*, 2003, 39, 1019-1029.
41. A. I. Fiaschi, A. Cozzolino, G. Ruggiero and G. Giorgi, *Eur Rev Med Pharmacol Sci*, 2005, 9, 361-367.
42. J. M. Estrela, A. Ortega and E. Obrador, *Crit Rev Clin Lab Sci*, 2006, 43, 143-181.
43. G. Wu, Y. Z. Fang, S. Yang, J. R. Lupton and N. D. Turner, *J Nutr*, 2004, 134, 489-492.
44. J. Gajewska, M. Szczypka, K. Pych, A. Borowka and T. Laskowska-Klita, *Neoplasma*, 1994, 42, 167-172.
45. K. M. Schultz, A. D. Baldwin, K. L. Kiick and E. M. Furst, *Macromolecules*, 2009, 42, 5310-5316.
46. K. G. Robinson, T. Nie, A. D. Baldwin, E. C. Yang, K. L. Kiick and R. E. Akins, Jr., *J Biomed Mater Res A*, 2012, 100, 1356-1367.
47. C. C. Lin and K. S. Anseth, *Pharm Res*, 2009, 26, 631-643.
48. E. A. Phelps, N. O. Enemchukwu, V. F. Fiore, J. C. Sy, N. Murthy, T. A. Sulchek, T. H. Barker and A. J. Garcia, *Adv Mater*, 2012, 24, 64-70, 62.
49. Y. Lei and T. Segura, *Biomaterials*, 2009, 30, 254-265.
50. C. L. McGann, E. A. Levenson and K. L. Kiick, *Macromol Chem Phys*, 2013, 214, 203-213.

51. D. Gupta, C. H. Tator and M. S. Shoichet, *Biomaterials*, 2006, 27, 2370-2379.
52. L.-T. T. Nguyen, M. T. Gokmen and F. E. Du Prez, *Polym Chem*, 2013, 4, 5527-5536.
53. J. P. Danehy and Paramesw.Kn, *J Chem Eng Data*, 1968, 13, 386-&.
54. T. V. DeCollo and W. J. Lees, *J Org Chem*, 2001, 66, 4244-4249.
55. L. R. G. Treloar, *The physics of rubber elasticity*, Oxford University Press, 1975.
56. P. M. Gschwend and D. M. Imboden, *Environmental organic chemistry*, John Wiley & Sons, 2005.
57. Y. S. Jo, J. Gantz, J. A. Hubbell and M. P. Lutolf, *Soft Matter*, 2009, 5, 440-446.
58. P. J. Martens, S. J. Bryant and K. S. Anseth, *Biomacromolecules*, 2003, 4, 283-292.
59. R. G. Schoenmakers, P. van de Wetering, D. L. Elbert and J. A. Hubbell, *J Control Release*, 2004, 95, 291-300.
60. M. C. Branco, D. J. Pochan, N. J. Wagner and J. P. Schneider, *Biomaterials*, 2010, 31, 9527-9534.
61. J. Siepmann and N. A. Peppas, *Adv Drug Deliver Rev*, 2012, 64, 163-174.
62. J. Siepmann and F. Siepmann, *Int J Pharm*, 2008, 364, 328-343.
63. S. P. Zustiak and J. B. Leach, *Biotechnol Bioeng*, 2011, 108, 197-206.
64. A. Raza and C. C. Lin, *Macromol Biosci*, 2013, 13, 1048-1058.
65. S. Y. Choh, D. Cross and C. Wang, *Biomacromolecules*, 2011, 12, 1126-1136.

FIGURES

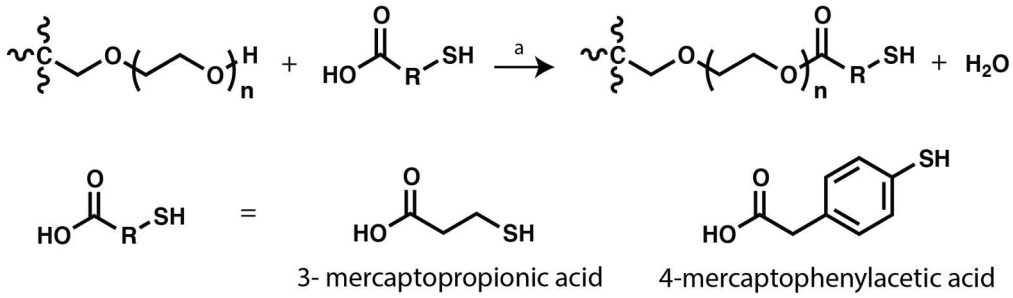

Scheme 1. Functionalization of 4-arm PEG. Schematic of the synthesis of thiol-functionalized PEG. (a: Toluene, PTSA, ~110 ^{0}C)

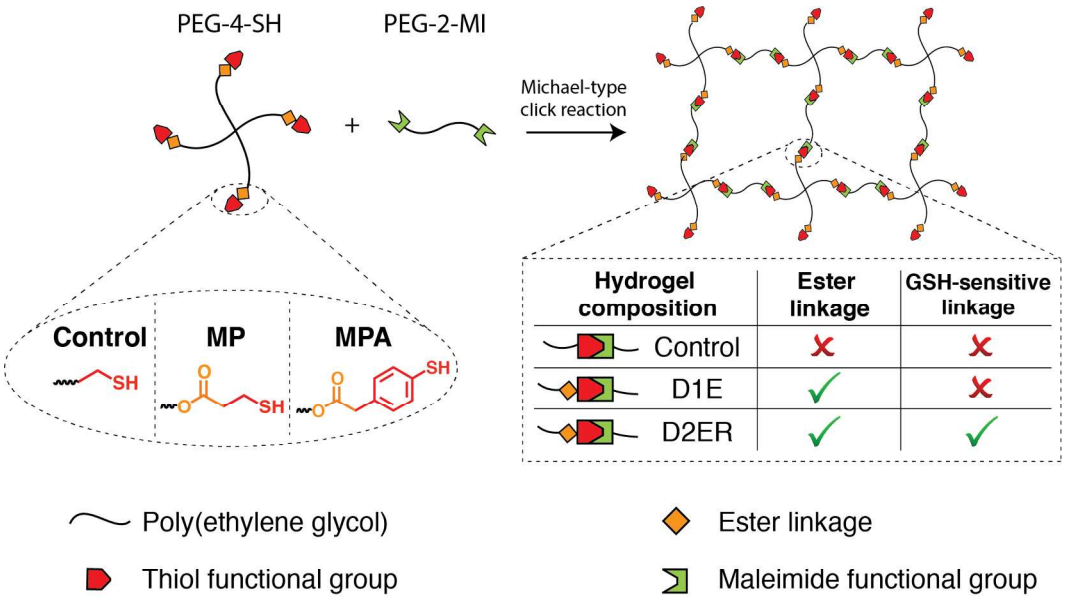

Fig. 1. Hydrogel formation via click reaction. Degradable PEG hydrogels were synthesized by Michael type addition reaction between thiol functionalized 4-arm PEG (PEG-4-SH) and maleimide functionalized linear PEG (PEG-2-MI). The thiol-functionalized macromers were synthesized by esterification of PEG using two different mercaptoacids (Scheme 1). The identity of the thiol was varied to tune the degradability of the hydrogels (**Control**: no degradable groups; **D1E**: one degradable group per crosslink (i.e., ester linkage); and **D2ER**: two degradable groups per crosslink (i.e., ester and reducing environment susceptible click = linkages).

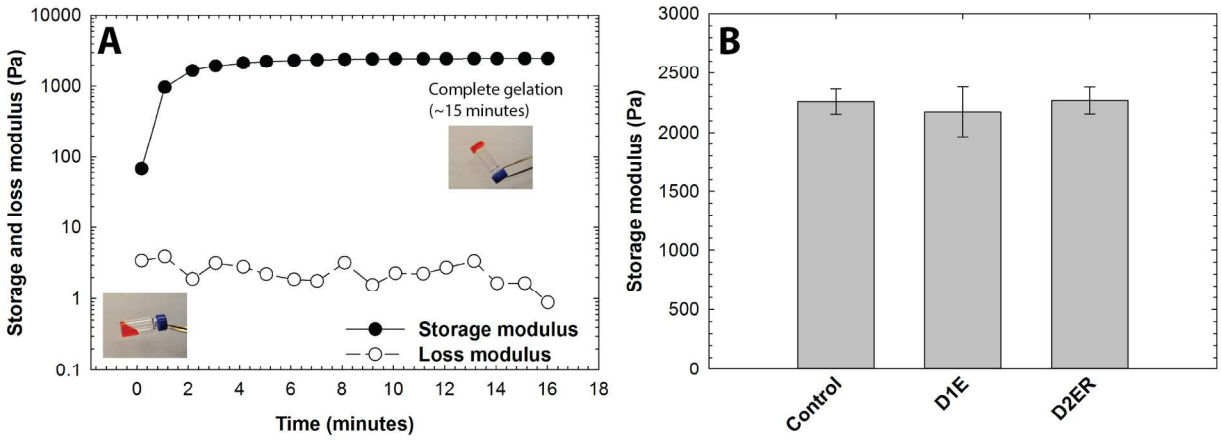

Fig. 2. Modulus evolution during hydrogel formation. A) Time-sweep measurements on an oscillatory rheometer were utilized to monitor hydrogel formation (**D2ER** hydrogel shown). Although formation of a gel is clearly observed, samples polymerize too quickly for measurement of the gel point with rheometry. To estimate the time to initial gelation, the tube-tilt method was utilized (inset images), where faster gelation was observed for **D2ER** (~20 s) as compared to **Control** (~40 s) and **D1E** (~35 s) hydrogels. For better visual assessment, Allura Red AC dye was added to the precursor solution (0.5 mg/ml) for tube-tilt measurements. **B)** Irrespective of the identity of the thiol used for the hydrogel formation, the storage moduli for all three hydrogels post-gelation were statistically similar, indicating similar structural and mechanical properties. The data shown illustrate the mean (n = 3), with error bars showing the standard error.

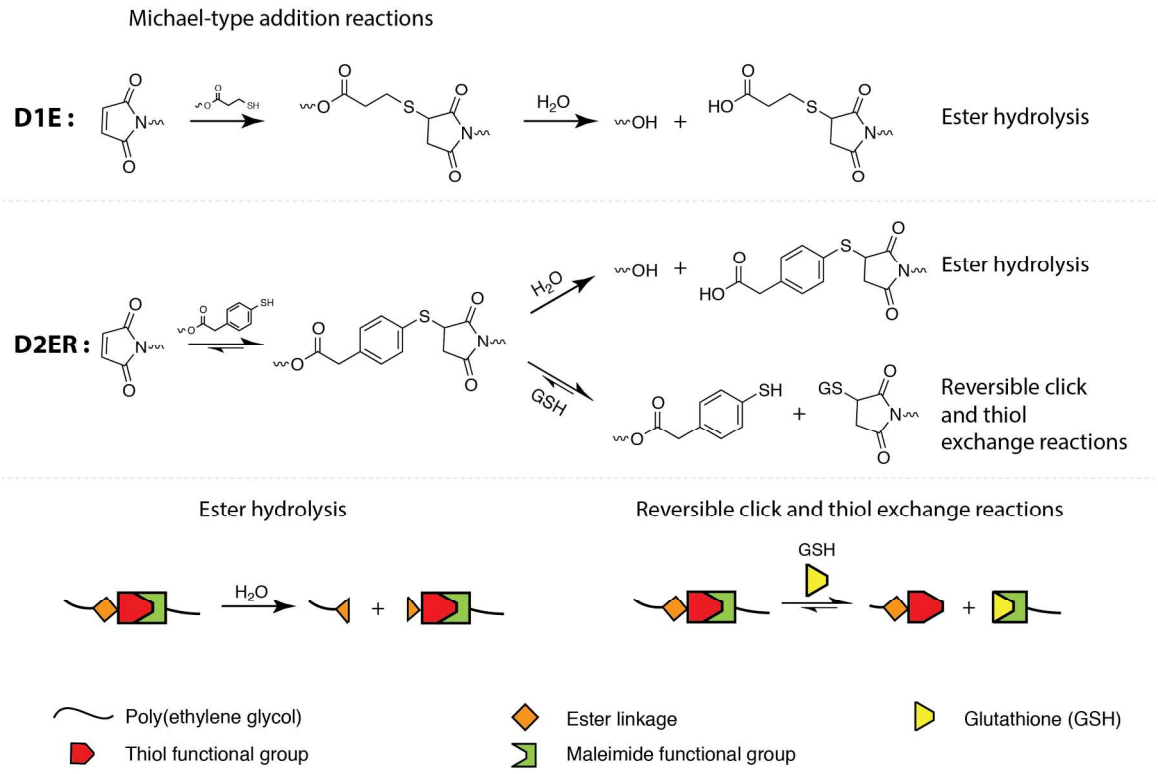

Fig. 3. Multimode hydrogel degradation. Schematic of the click bond cleavage and thiol exchange reaction of thioether succinimide linkages under a glutathione (GSH) reducing microenvironment and by ester hydrolysis. The **D1E** hydrogels can only undergo degradation by ester hydrolysis. **D2ER** hydrogels can undergo degradation by ester hydrolysis and by thiol exchange reactions, owing to the presence of arylthiol-based thioether succinimide linkages. Owing to the lack of degradable functional groups, control hydrogels do not degrade in aqueous reducing microenvironments. The rate and extent of the click bond cleavage depends on the Michael donor reactivity and thiol pK_a.

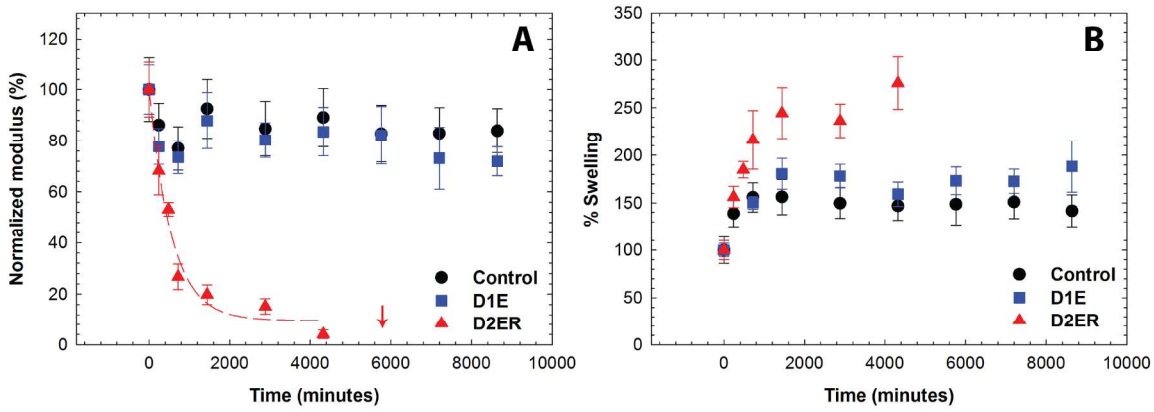

Fig. 4. Hydrogel degradation in reducing microenvironment by cleavage of click bonds. Degradation of the hydrogel in a thiol-rich reducing microenvironment (10 mM GSH) was studied by monitoring **A)** the storage modulus and **B)** % volumetric swelling at discrete time points. All compositions exhibit an initial change in properties over 24 h as equilibrium swelling occurs. Due to the presence of the arylthiol-based thioether succinimide crosslinks, **D2ER** hydrogels exhibited rapid bulk degradation by click cleavage and thiol exchange reactions. The arrow indicates the time point when reverse gelation was observed. **D1E** and **Control** hydrogels were relatively stable during the experimental time frame due to the absence of GSH-sensitive crosslinks. The data shown illustrate the mean (n = 6), with error bars showing the standard error.

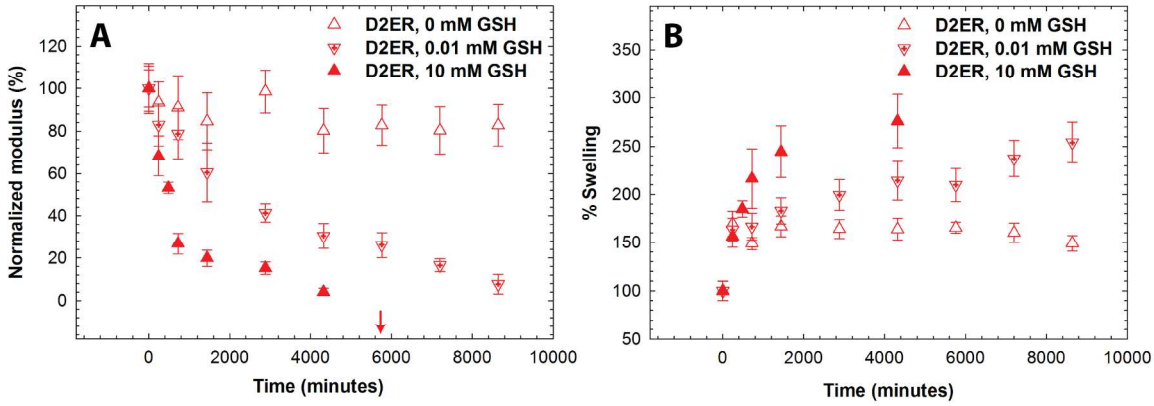

Fig. 5. Influence of GSH concentration on hydrogel degradation. The effect of GSH concentration (0, 0.01, and 10 mM) on **D2ER** hydrogel degradation was studied by analyzing **A)** the decrease in the storage modulus, and **B)** the % volumetric swelling. The dependence of the decrease in moduli on GSH concentration indicates that the click cleavage and thiol exchange reaction is the dominant degradation mechanism for the **D2ER** hydrogels. The increase in volumetric swelling as a function of time before the reverse gel point confirms bulk degradation of hydrogels. The arrow indicates the time point when reverse gelation was observed for the 10 mM GSH condition. The data shown illustrate the mean (n = 6), with error bars showing the standard error.

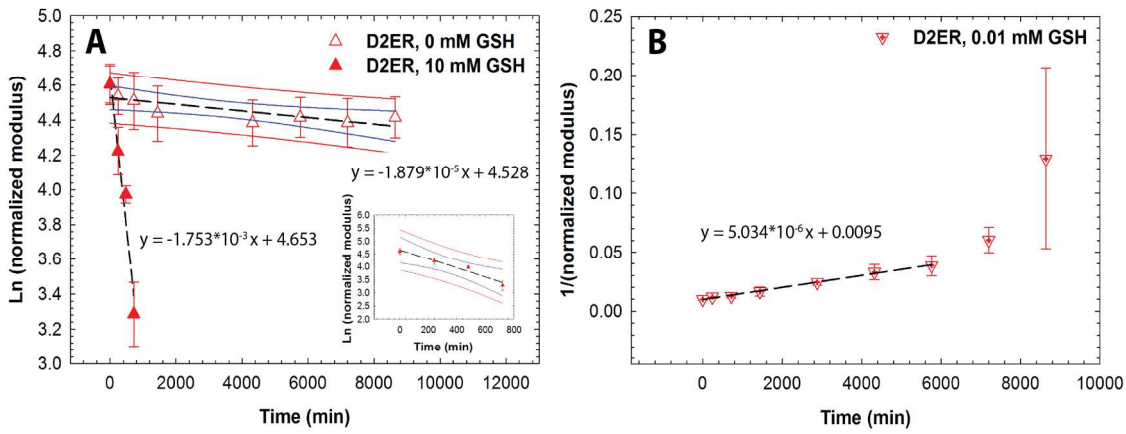

Fig. 6. Reducing environment-dependent degradation kinetics. A) D2ER hydrogels exhibited first order degradation kinetics in a strong reducing microenvironment (10 mM GSH), whereas limited degradation is observed in a thiol-lacking microenvironment (0 mM GSH), owing to the slow rate of ester hydrolysis. Data point for 0 mM GSH at 2880 minutes was identified as a significant outlier (Grubb's test, $p < 0.05$) and hence omitted during regression analysis. **B) D2ER** hydrogels followed second order reaction kinetics in a weak reducing microenvironment (0.01 mM GSH). Later time points were omitted during the regression analysis, due to large standard error, which can be attributed to experimental limitations when handling soft, more liquid-like degraded gels. As a whole, this study highlights the dependence of hydrogel degradation on GSH concentration. The data shown illustrate the mean ($n = 6$), with error bars showing the standard error. Black line indicates the linear fit using regression analysis. Blue and red lines indicate 95% confidence and prediction bands.

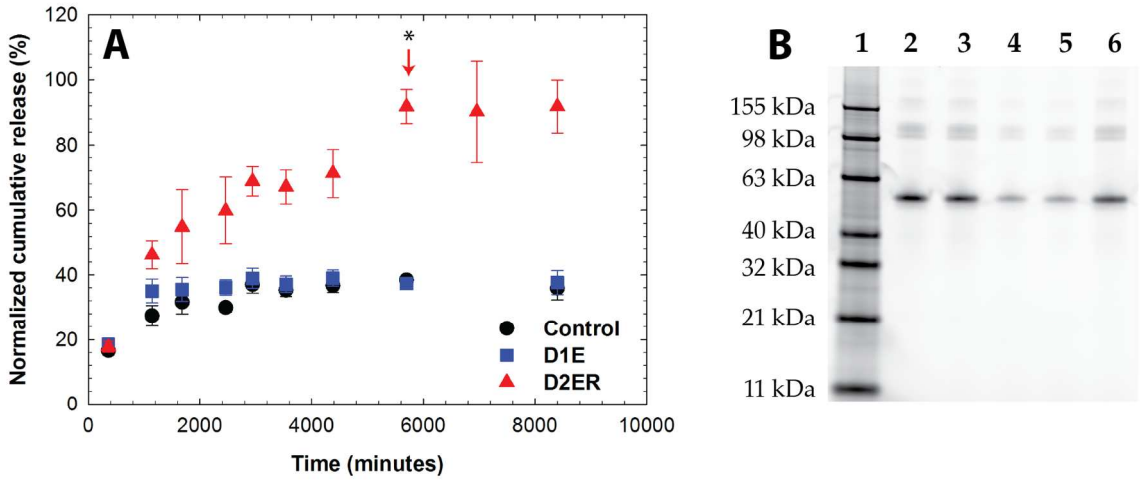

Fig. 7. Protein release in a reducing microenvironment. A) Release of a fluorescently-labeled model cargo protein, bovine serum albumin (BSA-488), was monitored using fluorometry. The arrow indicates the time point when reverse gelation (complete gel dissolution) was observed for the **D2ER** hydrogel. While some protein is initially released from all compositions upon gel equilibrium swelling, release from the **Control** and **D1E** hydrogels after this is minimal, owing to no or slow hydrolytic degradation, respectively, over the time course of the experiment. Substantial, statistical differences ($p < 0.05$ for time points after complete hydrogel degradation) in protein release are observed as the **D2ER** hydrogel rapidly degrades by the click cleavage and thiol-mediated exchange mechanism in addition to hydrolytic degradation. Differences in the release profile of BSA-488 from **D2ER**, **D1E**, and **Control** hydrogels highlight that the delivery of cargo molecules is controlled by hydrogel degradation. The data shown illustrate the mean ($n = 6$), with error bars showing the standard error. **B)** SDS-PAGE analysis of released protein. Lane 1: protein ladder; Lane 2: free BSA-488; Lane 3: free BSA-488 suspended in reducing microenvironment (10

mM GSH/PBS) with hydrogel precursor solution; Lane 4, 5, 6: supernatant after protein release from **Control**, **D1E**, and **D2ER** hydrogel, respectively. No major differences in the locations of the free BSA and released BSA band are observed, confirming that the protein remained intact during encapsulation and release. Further, analysis of the band intensity by densitometry further supports the relative amounts of protein released from each gel composition as determined by fluorescence (**Control**: ~33%; **D1E**: ~36%; and **D2ER**: ~90%).